

Supplementary information

Formation of nanostructured cellulose stearoyl esters via nanoprecipitation

Andreas Geissler,^a Markus Biesalski,^a Thomas Heinze,^b Kai Zhang^{a,*}

^a Ernst-Berl-Institute for Chemical Engineering and Macromolecular Science, Technische Universität Darmstadt, Petersenstr. 22, D-64287 Darmstadt, Germany

^b Center of Excellence for Polysaccharide Research, Institute of Organic Chemistry and Macromolecular Chemistry, Friedrich Schiller University of Jena, Humboldtstr. 10, D-07743 Jena, Germany

* Corresponding author

Tel.: +49 6151 16 75831; Fax: +49 6151 16 72931

Email: zhang@cellulose.tu-darmstadt.de

FT Raman

FT Raman spectra of the samples in small aluminium discs were recorded on a Bruker MultiRam spectrometer (Bruker Optics, Ettlingen, Germany) with a Ge diode as detector that is cooled with liquid nitrogen. A cw-Nd:YAG-laser with an exciting line of 1064 nm was applied as light source for the excitation of Raman scattering. The spectra were recorded over 3500-150 cm^{-1} using an operating spectral resolution of 3 cm^{-1} and a laser power output of 100 mW. A double analysis per 200 scans was carried out and an average Raman spectrum was formed afterwards. The baseline of the spectra was corrected using the method ‘concave rubber band algorithm’ with 200 baseline points and 50 iterations.

Results: Comparing the FT Raman spectrum of cellulose and CSE1 (Figure S2), it is visible that the bands ascribed to vibrations of cellulose backbones are strongly decreased, such as at 1380, 1122 and 1096 cm^{-1} ,^{1,2} while several new bands emerge due to the introduction of stearoyl groups in cellulose chains. The bands at 2882 and 2849 cm^{-1} are attributed to CH_2 -groups of stearoyl groups, while the signal at 2725 cm^{-1} is derived from the vibrations due to interactions between methyl groups and the overtones of their deformation vibrations.³ The weak band at 1749 cm^{-1} is due to C=O stretching vibrations of esters,⁴ and the bands at 1439 as well as 1297 cm^{-1} are attributed to the deformation vibrations of C-H as well as C-C groups in stearoyl groups, respectively.³

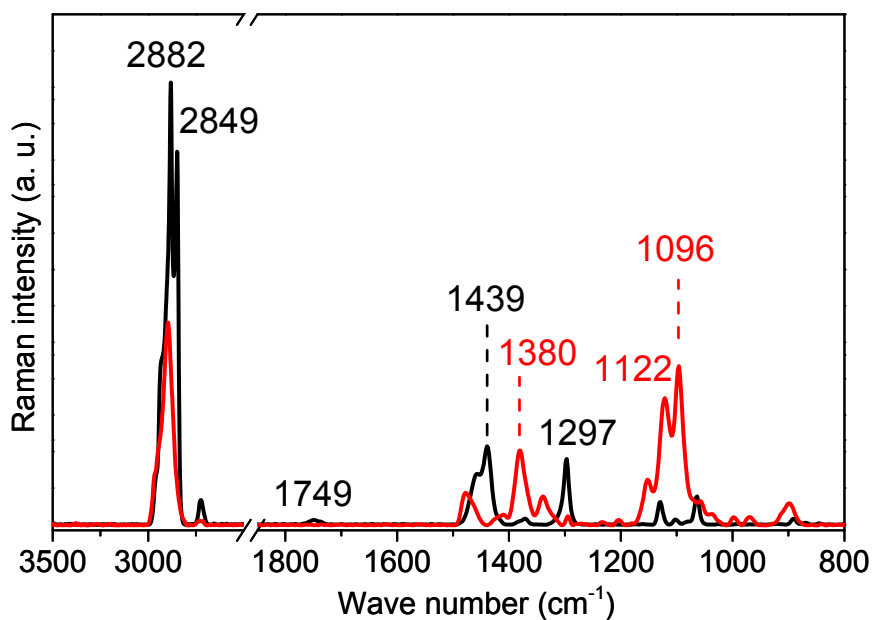


Figure S1. FT Raman spectrum (3500-800 cm^{-1}) of (a) microcrystalline cellulose and (b) CSE1 at room temperature.

¹³C NMR spectroscopy

The liquid-state ¹³C NMR spectra of cellulose stearoyl esters in deuterated benzene were recorded at RT on Bruker DRX 500 spectrometer (Bruker, Biospin GmbH, Ettlingen) with a frequency of 125.7 MHz, 30° pulse length, 0.88 s acq. time and a relaxation delay of 0.4 s. Scans of up to 12000 were accumulated.

Results: A typical ¹³C NMR spectrum of CSE in deuterated benzene shows characteristic chemical shifts due to cellulose backbone between 60-105 ppm (Figure 1). The signals between 10 and 60 ppm are assigned to the carbons in aliphatic chains.^{5,6} Chemical shifts between 170 and 175 ppm are typical for carbons in C=O-groups which are covalently bound to AGU.⁷ Three separate signals at 173, 172.2 and 171.9 ppm are visible and they are attributed to the carbons in C=O-groups at C6, C3 and C2-position of the AGU, respectively.^{6,8}

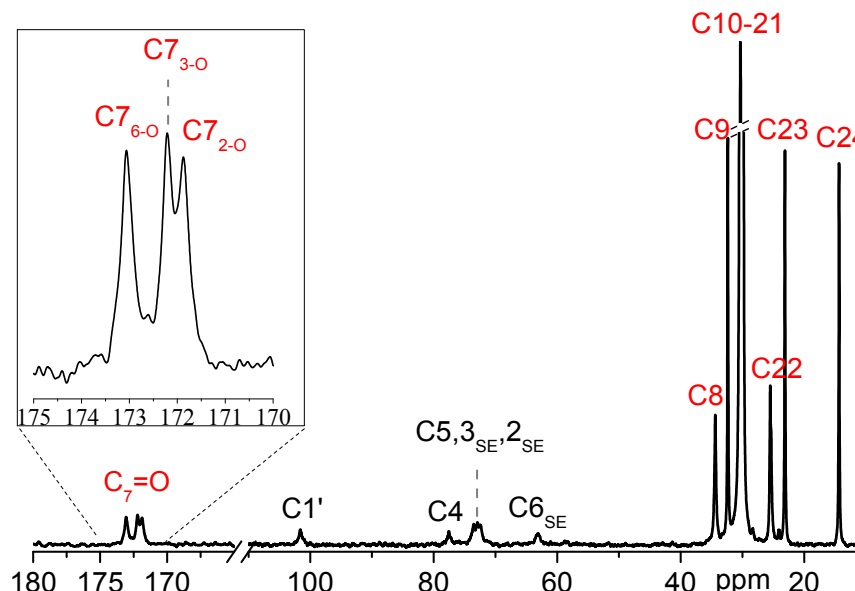


Figure S2. ¹³C NMR spectrum (180-10 ppm) of CSE in deuterated benzene.

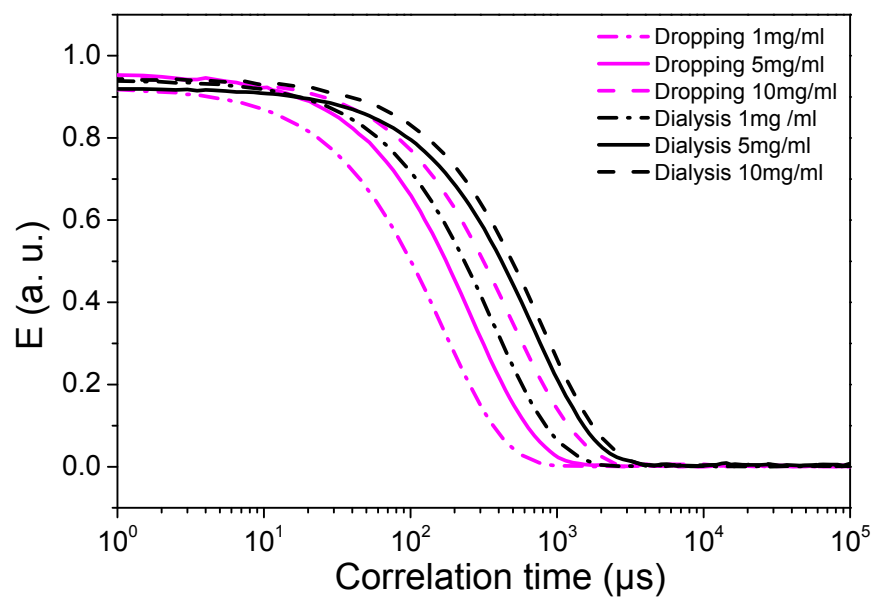


Figure S3. Autocorrelation curves of NPs from CSE2 via nanoprecipitation through dropping or dialysis route.

Table S1. ζ -potentials of a few NPs from corresponding CSE solutions of 5 mg/ml

NPs	ζ -potential
CSE1	-45.7±0.6
CSE2	-47.4±0.4
CSE3B	-46.7±0.3

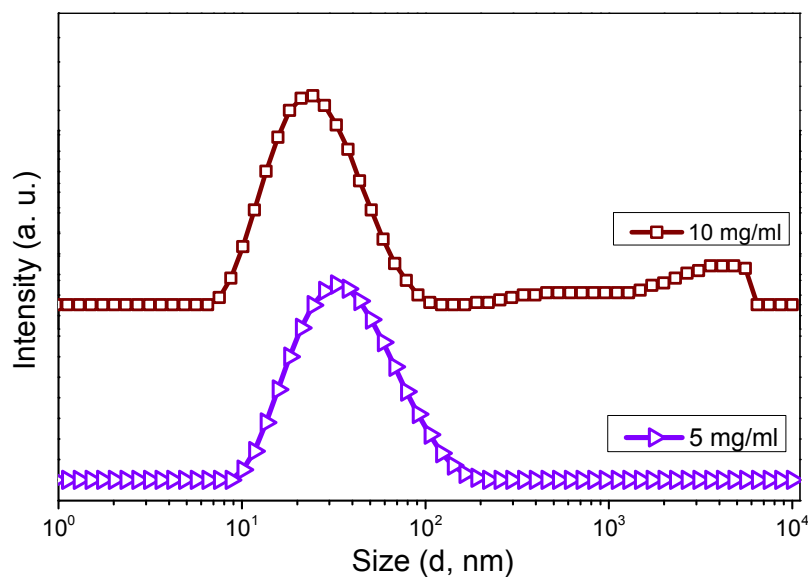


Figure S4. DLS of CSE2 solutions in THF of the concentrations 5 and 10 mg/ml.

Fluorescent microscopic images were captured on an Olympus BX60 fluorescent microscope (Olympus Deutschland GmbH, Hamburg, Germany) equipped with an Olympus XM10 camera. The excitation and emission wavelength were 541 and 572 nm, respectively. An exposure time of 20 ms was applied. Image analysis was performed using MAGIX Foto & Grafik Designer 2013 (Magix Software GmbH, Berlin, Germany).

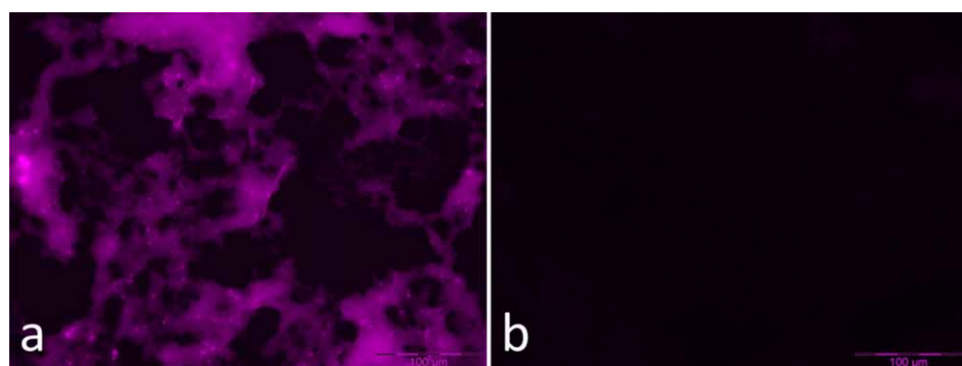


Figure S5. Fluorescent microscopic images of NPs after the dropping nanoprecipitation of CSE solution containing Rhodamine B of the saturated concentration: (a) NPs after the dialysis in water and (b) the same NPs after washing with ethanol.

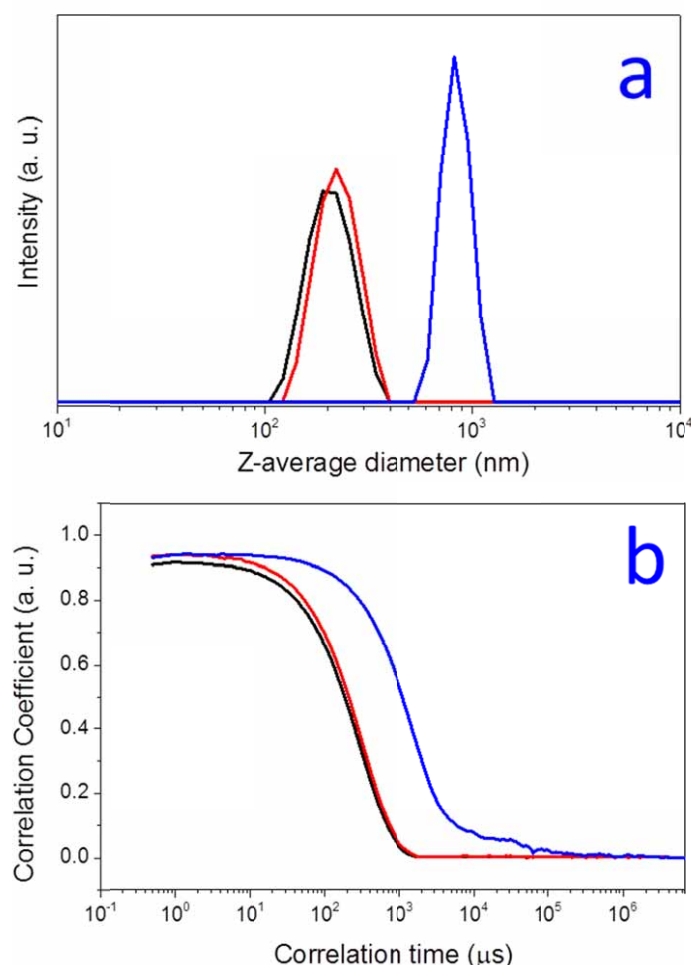


Figure S6. DLS size distribution curves and correlation curves of CSE-NP1 (black), NP1-Dr-RhB (red) and NP1-Di-RhB (blue).

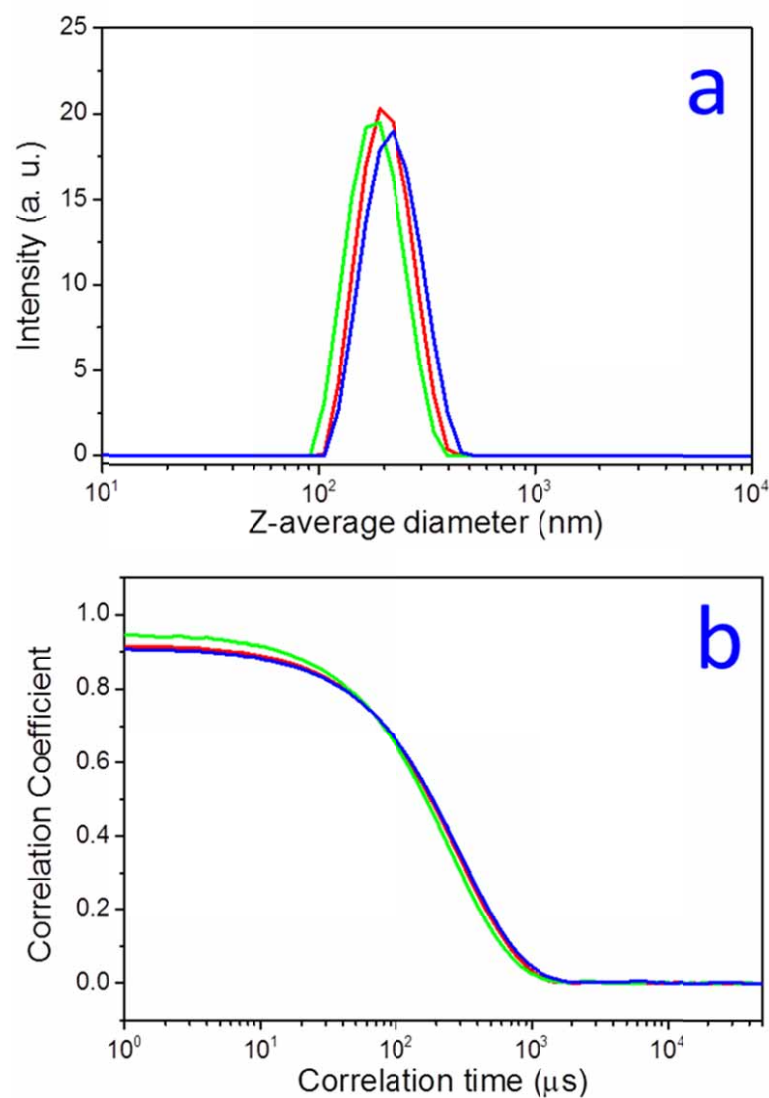


Figure S7. DLS of aqueous suspension of NPs from CSE solutions of 5 mg/ml via standard dropping procedure and modified dropping procedures. Red: standard dropping procedure (NP1), green: standard dropping procedure without stirring (NP1-NS), blue: addition of large volume via pouring (NP1-Po).

Table S2. Z-average diameters and PDI of NPs from CSE1 solutions of diverse concentrations after a storage at 4°C for 50 d or a treatment at 75°C for 15 min

Samples		Size (d, nm)	Shrinkage ratios (%)	PDI
CSE1 of 0.1 mg/ml	Fresh	139±0.5		0.143
	4°C for 50 d	108.4±1.2	22%	0.062
	15min 75°C	97.9±1.1	29.6%	0.07
CSE1 of 1 mg/ml	Fresh	163.1±0.7		0.069
	4°C for 50 d	153.9±1.2	5.6%	0.103
	15min 75°C	142.7±0.9	12.5%	0.046
CSE1 of 5 mg/ml	fresh	206.9±1.1		0.057
	4°C for 50 d	201.3±0.5	2.7%	0.064
	75°C for 15 min	201.7±2.3	2.5%	0.041
	1 h 95°C	195.9±0.5	5.3%	0.055
CSE1 of 10 mg/ml	Fresh	392.7±5.3		0.063
	4°C for 50 d	377.5±3.8	3.9%	0.06
	75°C for 15 min	386.1±6	1.7%	0.208

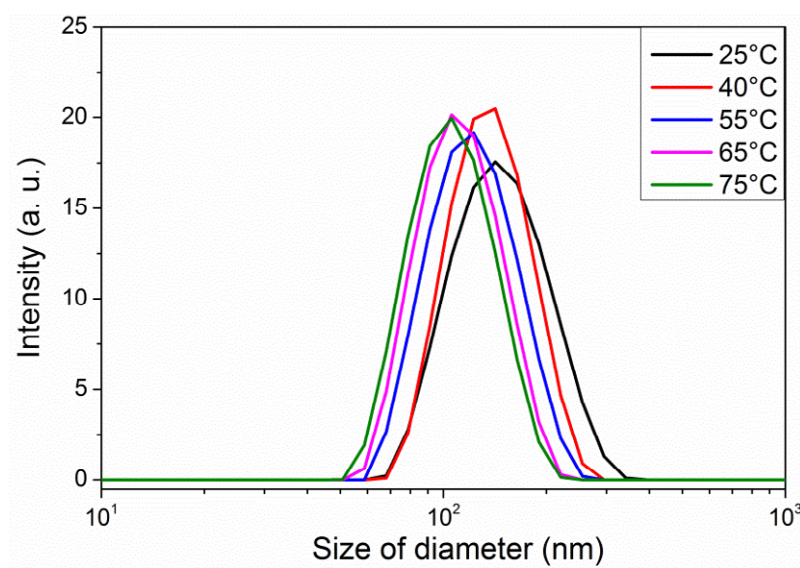


Figure S8. Representative DLS curves of heating treatment of freshly prepared NPs suspension at diverse temperatures (25, 40, 55, 65 and 75°C). NPs were prepared using 0.1 mg/ml solution of CSE1 in THF.

DSC measurements were done on a computer aided TA Instruments DSC Q1000 (TA Instruments, Eschborn, Germany). Dried N₂ gas was purged with a constant flow rate during the measurement. The temperature reading and caloric measurements were calibrated using indium and blue sapphire as the standard.

Results: A signal at ~56°C was observed and it is related to the decrystallization process of crystal structure that was formed by the stearoyl groups in CSE.^{9,10}

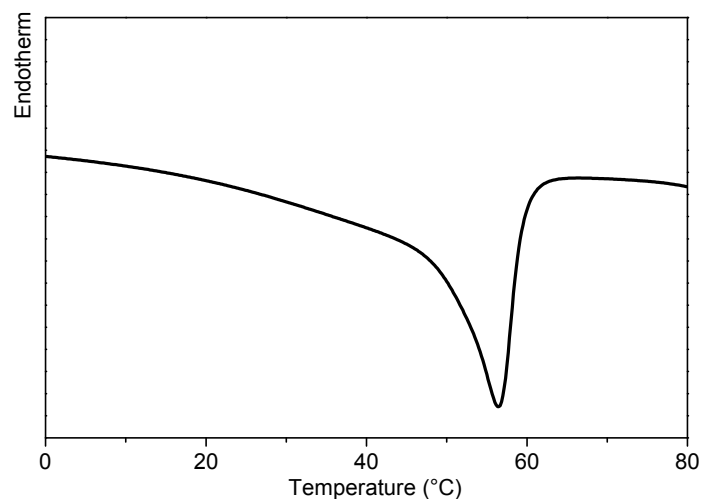


Figure S9. DSC of CSE1.

Table S3. Advancing and receding angles of water drops (0.4 µl) on superhydrophobic and hydrophobic surface.

Substrates	θ_A (°)	θ_R (°)	$\Delta\theta$ (°)
Superhydrophobic surface (freshly prepared)	156±2	153±1	3
Hydrophobic surface (after treatment at 70°C)	107±2	72±3	35

References

1. K. Schenzel, S. Fischer, *Cellulose*, 2001, **8**, 49-57.
2. J. H. Wiley, R. H. Atalla, *Carbohydr. Res.*, 1987, **160**, 113-129.
3. G. Socrates, *Infrared and Raman characteristic group frequencies*, 3rd. Edn.; Wiley: England, 2001.
4. K. Zhang, A. Feldner, S. Fischer, *Cellulose*, 2011, **18**, 995-1003.
5. T. Liebert, J. Wotschadlo, P. Laudeley, T. Heinze, *Biomacromolecules*, 2011, **12**, 3107-3113.
6. Y. Tezuka, Y. Tsuchiya, *Carbohydr. Res.*, 1995, **273**, 83-91.
7. T. Heinze, T. Liebert, K. S. Pfeiffer, M. A. Hussain, *Cellulose*, 2003, **10**, 283-296.

8. P. Dais, A. S. Perlin, *Carbohydr. Res.*, 1988, **181**, 233-235.
9. J. E. Sealey, G. Samaranayake, J. G. Todd, W. G. Glasser, *J. Polymer Sci. B Polymer Phys.*, 1996, **34**, 1613-1620.
10. C. Vaca-Garcia, G. Gozzelino, W. G. Glasser, M. E. Borredon, *J. Polymer Sci. B Polymer Phys.*, 2003, **41**, 281-289.